

Electron Transfer and Electron Excitation Processes in 2,5-Diaminoterephthalate Derivatives with Broad Scope for Functionalization

Aleksandra Markovic, Leon Buschbeck, Thorsten Klüner, Jens Christoffers, and Gunther Wittstock*^[a]

Derivatives of 2,5-diaminoterephthalate (DAT) are efficient fluorescence dyes that are also redox-active, thus allowing for the electrochemical manipulation of spectral properties. The electrochemical behaviour of seven DAT derivatives was studied by cyclic voltammetry in dichloromethane. In the absence of a proton donor, DATs should be oxidized in two one-electron steps. The first step is usually quasi-reversible while the second step is either quasi-reversible or irreversible. Some electro-

chemical properties such as the formal potentials and the ratio between the anodic and the cathodic current were determined from the cyclic voltammograms. Correlation between the formal potential of first oxidation and the absorption or the fluorescence emission wavelengths are established for this specific type of dyes. These correlations were confirmed with density functional theory calculations.

1. Introduction

The synthesis of the dialkyl 2,5-diaminoterephthalate (DAT) was first published by von Baeyer in 1886.^[1] The structural motif is a chromophore which contains two carboxylate and two amino functions (Figure 1). Most DAT derivatives are deeply orange to red colored compounds^[2,3] and usually exhibit strong fluorescence.^[4] Even though DATs have been known since the beginning of the last century, literature about them is limited compared to other classes of dyes. Interestingly, the DAT motif allows easy functionalization with up to four different effector units.^[5] These properties are attractive for application as a probe in life sciences and materials science.^[5] These compounds are obtained by reactions of succinyl succinates with amines followed by aerobic oxidation.^[5]

Monofunctionalized DATs have been reported as fluorescence sensor for hydrogen peroxide detection^[6] or as fluorescent probes covalently bound to proteins or other biomolecules.^[5] For example, the maleimide group can be used as functional group for the ligation of a thiol moiety at the surface of proteins.^[7,8] It is of particular value that the fluorescence quantum yield of this dye-protein conjugate is orders of magnitude higher than that of the dye itself, such dyes are called “turn on probes”.^[9–17] DATs can also be

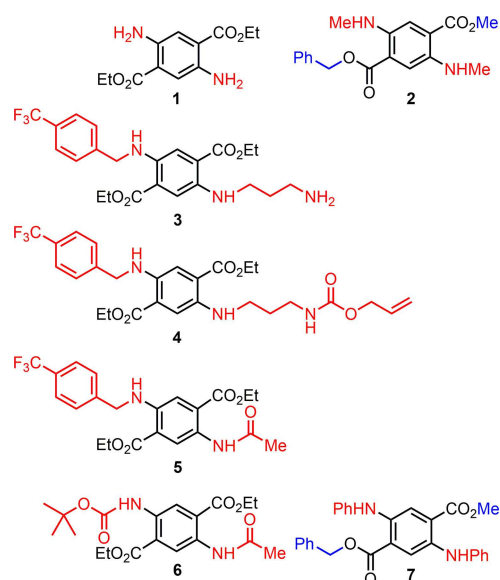


Figure 1. Structures of DAT derivatives investigated in this study (*N*-substitutions that influence the electrochemical behaviour are marked in red; ester groups different from ethyl are marked in blue).

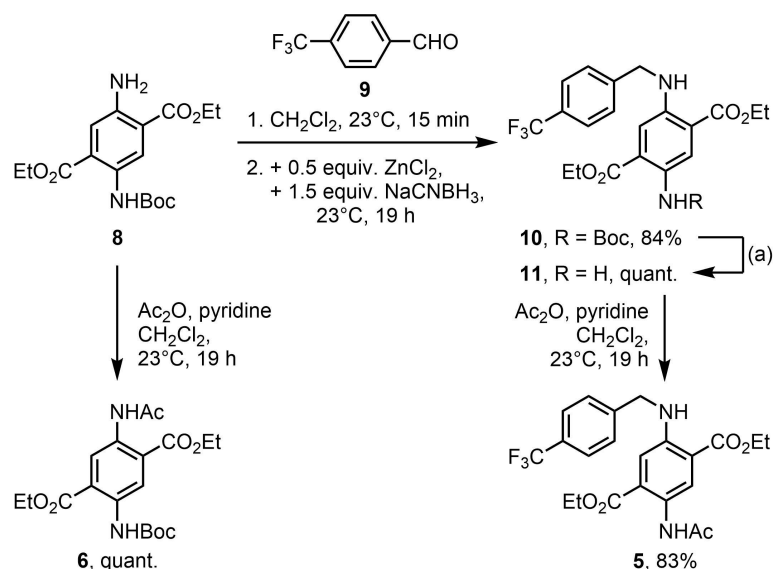
monofunctionalized for copper-free click reactions^[18] with the cyclooctyne unit.^[19] Fullerene (C₆₀) can be easily ligated to these dyes by cycloaddition reactions. Several dye-fullerene conjugates, so called dyads, have been synthesized in the past years.^[20–24] The dyads have been constructed and investigated with the purpose to mimic natural photosynthesis and to understand fundamentals of photoinduced electron and energy transfer processes.^[25–27]

DATs for biochemical applications have also been prepared as turn-on probes, where the effect of higher fluorescence quantum yield was observed upon conjugated addition of benzylmercaptane.^[28] The DAT building block has been used for

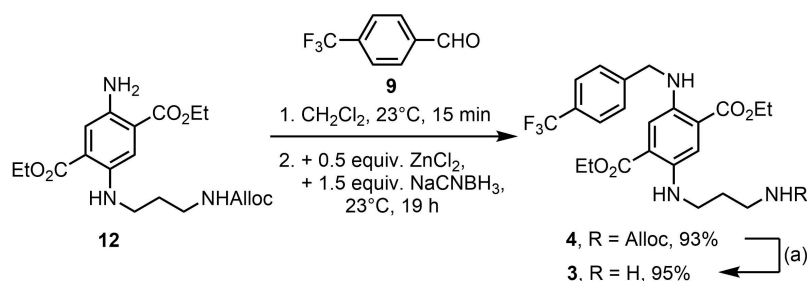
[a] A. Markovic, Dr. L. Buschbeck, Prof. Dr. T. Klüner, Prof. Dr. J. Christoffers, Prof. Dr. G. Wittstock
Carl von Ossietzky University Oldenburg, School of Mathematics and Science, Chemistry Department, D-26111 Oldenburg, Germany
E-mail: wittstock@uol.de

Supporting information for this article is available on the WWW under <https://doi.org/10.1002/open.201900138>

© 2019 The Authors. Published by Wiley-VCH Verlag GmbH & Co. KGaA. This is an open access article under the terms of the Creative Commons Attribution Non-Commercial NoDerivs License, which permits use and distribution in any medium, provided the original work is properly cited, the use is non-commercial and no modifications or adaptations are made.



Scheme 1. Preparation of compounds **5** and **6**; conditions: (a) TFA/ CH_2Cl_2 (1:1), 23°C , 19 h. Boc = *tert*-butoxycarbonyl, Ac = acetyl, TFA = trifluoroacetic acid.



Scheme 2. Preparation of compounds **3** and **4**; conditions (a) 0.05 eq $\text{Pd}(\text{PPh}_3)_4$, 5.0 eq morpholine, abs. CH_2Cl_2 , 23°C , 1 h. Alloc = allyloxycarbonyl.

studying protein-protein interactions, such as the dimerization of two molecules of recoverin.^[19] DATs were also used as ligands for synthesis of metal complexes^[29,30] and applied as linker compounds for metal organic frameworks (MOF).^[31] Given this broad range of applications, it is important to understand the redox properties of DAT derivatives because they may be exploited in addition to their fluorescence and binding properties. This is even more important as the merging of electrochemical and fluorescence experiments is finding more and more attention.^[32]

DATs could be regarded as *p*-phenylenediamine derivatives whose redox properties should be similar to hydroquinones, for which two subsequent one-electron oxidations have been reported in aprotic solutions.^[33–36] To date, no literature is available about the electrochemical behaviour of DAT derivatives in aprotic media. Here we study the electrochemical properties of the seven DAT derivatives with different functional units (Figure 1).

2. Results and Discussion

The preparation of DAT derivatives **5** and **6** started from mono-carbamate protected diethyl DAT **8** (Scheme 1). Compound **1**

was accessed in three steps from diethyl succinate *via* compound **1** according to Wu and co-workers.^[37] The primary amino group of compound **8** was amidated with Ac_2O -pyridine to furnish the bis-amide **6** in quantitative yield. Reductive amination of compound **8** with trifluoromethylated benzaldehyde **9** was accomplished with a mixture of ZnCl_2 and NaCNBH_3 ^[38] yielding the respective *N*-benzylated compound **10** in good yield. After subsequent *N*-Boc-deprotection with TFA (product **11** in quantitative yield) the primary amino function was also amidated with Ac_2O -pyridine to give the mono-amide **5** in 83% yield.

The preparation of products **3** and **4** started from compound **12** (Scheme 2), which was accessed from compound **8** in two steps (reductive amination with *N*-Alloc-3-aminopropanal and subsequent *N*-Boc-deprotection) as reported recently.^[39] Reductive amination with trifluoromethylated benzaldehyde **9** was accomplished as above and furnished product **4** in 93% yield. The alloc-protective group was then cleaved (95% yield of product **3**) in a palladium catalyzed allylic substitution reaction with morpholine as a scavenger of the allylic cation.^[40,41]

The investigated DAT derivatives have different substituents that influence the electron density and thus modify the property of the diamine/diimine group marked red in Figure 1.

We here used these compounds to uncover a systematic variation of the DAT electrochemical and spectroscopic properties.

Cyclic voltammetry at a GC electrode in the CH_2Cl_2 solution was used to determine the formal potentials ($E^{\circ'}$). Typical voltammograms, recorded at the scan rate 0.1 V s^{-1} are shown in Figure 2. $E^{\circ'}$ values extracted from these voltammograms are summarized in Table SI-2. The formal potentials $E^{\circ'}$ are independent of the scan rate. The cyclic voltammograms of the DAT derivatives at GC electrode at all scan rates ν between

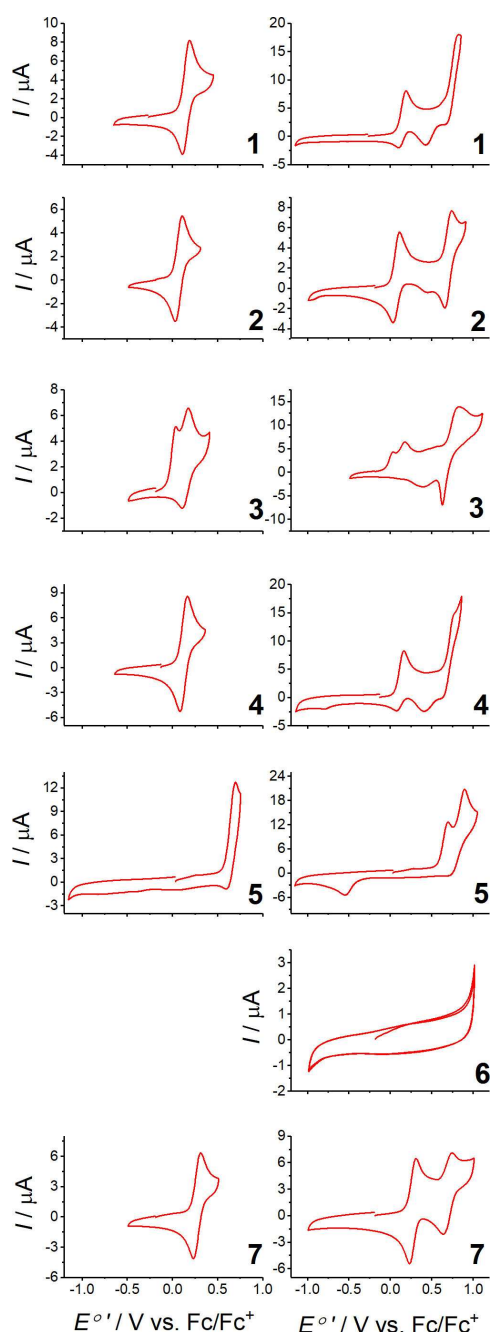


Figure 2. Cyclic voltammetry of DAT derivatives (0.3 mM concentration) in CH_2Cl_2 and 0.1 M Bu_4NClO_4 as supporting electrolyte, $\nu = 100 \text{ mV/s}$ in two different potential ranges; the compound number is given in each diagram (right lower corner).

0.01 V s^{-1} and 1 V s^{-1} show different appearance of the cathodic and the anodic peaks depending on the particular molecular structure. In most cases, the first peak is quasi-reversible while the second peak is quasi-reversible or irreversible. This is concluded from the dependence of ΔE_p on ν as well as by the change in I_{pa}/I_{pc} with ν . The current functions of the scan rate ($I_p/\nu^{1/2}$) and the ratio of anodic to cathodic peak currents (I_{pa}/I_{pc}) changes with ν for most of the investigated compounds, especially in extended potential range (SI-8, Table SI-1).

The exception of compound 7 for the general trends from the other DAT derivatives is understandable as it is the only derivative in which two phenyl groups are directly attached to the amino functions thus altering considerable the electronic properties of the redox active group. Compound 1 has two unsubstituted aromatic amino groups as redox active moieties (Figure 1). In the potential range from -0.65 V to 0.45 V , there is one pair of oxidation and reduction peaks ($E^{\circ'} = 0.15 \text{ V}$) where a radical cation is formed and re-reduced to the initial compound in the negatively going scan. When the potential range is extended to $1.00 \text{ V vs. Fc/Fc}^+$, a second oxidation peak appears at 0.82 V accompanied by a reduction peak at 0.43 V . With the appearance of the second oxidation peak, the magnitude of the reduction current of the first redox couple is decreased indicating consumption of the oxidation product by an irreversible reaction.

In compound 2, the redox active DAT moiety is substituted by two methyl groups. In the potential range from -0.5 V to 0.3 V , one oxidation peak is observed at $E_{pa} = 0.11 \text{ V}$ and one reduction peaks occurs at $E_{pc} = 0.03 \text{ V}$ ($E^{\circ'} = 0.07 \text{ V}$). Only one electron is transferred, i.e. a radical cation is formed and reduced to the initial compound in the negatively going scan. From the parameters in Table SI-1 it is obvious that this is a quasi-reversible reaction. By extending potential range to $1.00 \text{ V vs. Fc/Fc}^+$, a second one-electron oxidation peak appears at 0.69 V . At lower scan rates, some side reaction occurs (additional reduction peak at 0.44 V , SI-8), but at scan rate larger than 0.5 V s^{-1} this feature disappears.

Compound 3 has trifluoromethylated benzylamino and 3-(aminopropyl)as substituents. This compound shows two oxidation peaks (0.03 V and 0.18 V) and one reduction peak (0.11 V) in the potential range between -0.5 V and 0.4 V . When the potential range is extended to $1.10 \text{ V vs. Fc/Fc}^+$, one more oxidation peak appears at 0.82 V and one narrow reduction peak at 0.63 V .

Compound 4 has trifluoromethylated benzylamino and 3-(allyloxycarbonylamino)-propylamino as redox active groups. In the potential range from -0.65 V to 0.40 V , there is a quasi-reversible redox couple with $E^{\circ'} = 0.13 \text{ V}$. When the potential range is expanded to 0.90 V , the compound behaves very similar to compound 1. All peaks on compound 4 are shifted by -0.02 V against the corresponding signals of compound 1.

Compound 5 has trifluoromethylated benzylamino and acetamino groups as substituents. There is one irreversible oxidation peak at 0.64 V in the potential range from

-1.15 V to 0.76 V . When the range is extended to 1.05 V , the second irreversible peak appears at 0.90 V , and one reduction peak appears at -0.54 V , which disappears after one

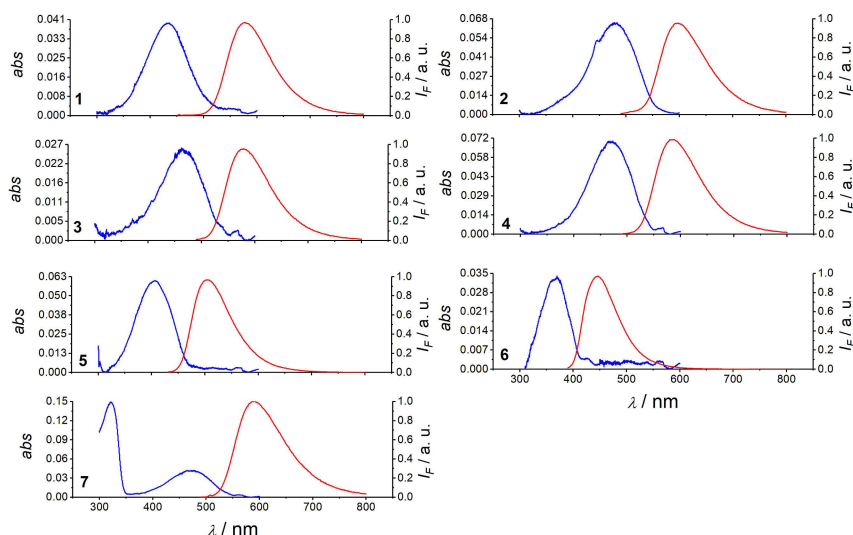


Figure 3. Absorption (in blue) and emission spectra (in red) of 9 μM DAT derivatives in ethanol; the compound number is given in each diagram (right lower corner).

cycle in potential range from -1.15 V to -0.15 V. Compound 6 structurally related to compound 5, with a trifluoromethylated benzylamino group is replaced by the *tert*-butyloxycarbonyl (Boc) group. This compound has no oxidation or reduction peaks in the potential range from -1.00 V to 1.05 V. One can see a slight current increase at around 0.95 V. This does not allow further conclusions as this potential range overlaps with the onset of solvent oxidation.

Compound 7 has two phenyl substituents directly at both amino groups of the DAT scaffold. Here, one quasi-reversible pair of peaks appears with $E^{\circ} = 0.27$ V in the potential range from -0.50 to 0.50 V. When the range is extended to 1 V, the second pair of peaks appears at 0.69 V. The second peak is also quasi-reversible.

Absorption and emission spectra are shown in Figure 3. As these compounds have electron-accepting or electron-donating substituents at both nitrogen atoms bound to the aromatic ring, shifts in absorption and emission wavelengths and changes in Stokes shifts are expected and are indeed observed (Table SI-2). Compound 1 carries two NH_2 groups and shows absorption and emission at 434 nm and 581 nm (Stokes shift of 147 nm). This compound exhibits the largest Stokes shift from all seven compounds investigated. Compound 2 has two electron-donating groups and the Stokes shift is lower (120 nm). Because of electron-donating groups, absorption and emission wavelengths are red-shifted to 478 nm and 598 nm. Compound 3 and 4 have similar electron-donating substituents. Therefore, their Stokes shift is the same (118 nm) although their absorption and emission wavelengths differ slightly (for compound 3 465 nm and 583 nm, for compound 4 467 nm and 587 nm). Compound 5 has one electron donating group and one electron-accepting group, so the Stokes shift is significantly lower (94 nm). Absorption and emission wavelengths are blue-shifted to 409 nm and 503 nm. Compound 6 has two electron-accepting groups, absorption and emission are even more blue-shifted than for compound 5 to 367 nm and 445 nm (Stokes

shift 87 nm). Compound 7 has two electron-donating groups and absorption and emission are in the same range as for compounds 3 and 4, 475 nm and 589 nm. The Stokes shift is slightly reduced to 114 nm compared to compounds 3 and 4 due to the influence of the groups attached to the ring.

Figure 4 shows a plot of the E° of the first oxidation vs. the wavelength of emission and absorption maximum for compounds 1, 2, 3, 4, 5 and 7. Full symbols are data obtained in ethanol (from spectra presented Figure 3) and empty symbols are data obtained in CH_2Cl_2 from ref.^[42,43]. Except for compound 7 and 1 the DAT derivatives exhibit a quite strict correlation between those quantities in both solvents. However, compound 7 is an exception because its phenyl substituents are directly attached to aromatic amino groups while all other aromatic substituents are separated by an aliphatic methylene group from the aromatic amine. The phenyl groups in compound 7

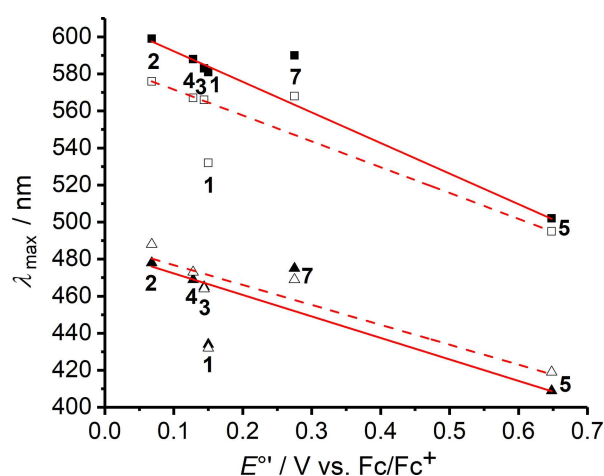


Figure 4. Correlation between formal potential in CH_2Cl_2 and wavelength of the absorption (\blacktriangle -in ethanol, \triangle -in CH_2Cl_2 ^[42,43]) and emission (\blacksquare -in EtOH, \square -in CH_2Cl_2 ^[42,43]) maxima for compounds 1–5 and 7.

stabilize the energy of the nonbonding orbital of nitrogen and increase the redox potential of compound **7** relative to the other DAT derivatives. The compound **1** is an exception in the correlation plot for the wavelength of absorption maximum in both solvents and in correlation for the wavelength of emission maximum in CH_2Cl_2 . This compound is carrying two NH_2 groups, the Stokes shift is significantly larger in spectra recorded in ethanol than for the compounds investigated (with substituents at the amino groups). As a consequence, the wavelength of the absorption maximum of compound **1** is significantly blue-shifted. Compound **1** has a significantly shifted wavelengths of maximum emission in CH_2Cl_2 compared to ethanol. Probably this shift is a consequence of the hydrogen bonding in ethanol. From these data, one can conclude that by measuring the fluorescence wavelengths, a prediction of the first redox potential is possible for DAT derivatives. However, all compounds in Figure 4 have at least one amino group, except for compound **6** which has two amido groups that are weaker donors than amines. Because of this, the E° of the first oxidation for compound **6** cannot be determined. The electronic delocalization is weakened causing a hypsochromic effect (Figure 3).

In order to understand the correlation between $\lambda_{\text{abs,max}}$, $\lambda_{\text{em,max}}$ and E° , we performed electronic structure calculations using density functional theory (DFT). Specifically, the DFT calculations allowed the estimation of the ionisation potential E_i [eV] for the DAT molecules by calculating the difference of total energies of the neutral and positively charged species. Absorption and emission wavelengths were obtained within time-dependent DFT (TDDFT). Despite our attempts to consider the relaxation of the nuclear position after the removal of an electron from the frontier orbitals by a geometry optimization of the excited states, the approach is of approximate nature as solvent effects were not considered. Furthermore, the (TD) calculations always exhibit an uncertainty due to the choice of the exchange-correlation functional. Due to these limitations, we cannot expect a precise agreement between calculated and measured data. However, correlation should appear when solvation effects and the error of the exchange correlation functional act similarly on the various DAT derivatives, their oxidation products and excited electronic states. Indeed, the correlation from the calculated results (Figure 5) show a reasonable agreement with the correlations obtained from the experimental results (Figure 4).

3. Conclusions

The 2,5-diaminoterephthalate (DAT) chromophore defines a molecular scaffold, which can be functionalized with up to four different effector groups which tailor the functionality of the compound. Such DATs with a variety of functional groups show different electrochemical properties depending on the groups attached to the DAT core. Surprisingly, DATs with completely different substituents at the DAT core (compound **1** and compound **4**) show completely identical redox behaviour with a difference in formal potential E° of only 0.02 V. DATs with

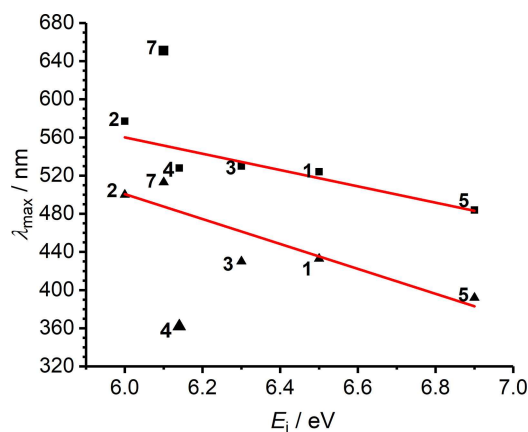


Figure 5. Correlation between calculated ionisation potential and calculated wavelength of the absorption (▲) and emission (■) maximum for compounds 1–5 and 7.

different effectors exhibit quite strict correlation between the E° of first oxidation and the wavelength of emission and absorption maximum. These results were also confirmed by DFT calculations. This correlation for wavelength of maximum absorption and emission holds with high precision for DATs with methyl or acetyl functionalities attached to the DAT scaffold of the compound. The electrochemical oxidation allows activation for the 1,4-addition. Due to the different formal potential of differently substituted derivatives, such a modification can also be followed via voltammetry, especially for surface-immobilized compounds, where monolayer coverages may not allow detection of absorption or fluorescence spectra. Overall surface-bound DAT derivatives may become an interesting anchor group for surface modification that can report their derivatisation by altered electrochemical and fluorescent properties.

Experimental Section

Materials

Compounds **1**,^[37] **2**^[22] and **7**^[28] were prepared according to literature procedures. All other compounds were prepared specifically for this study according to Scheme 1 (compounds **5** and **6**) and Scheme 2 (compounds **3** and **4**). Complete synthetic procedures as well as spectroscopic characterization can be found in the Electronic Supporting Information (ESI). The preparation of starting materials **8** and **12** was recently reported.^[39]

All solutions for physicochemical investigations were freshly prepared. The electrolytes were made-up with tetrabutylammonium perchlorate (Bu_4NClO_4 , 99.0%, Sigma Aldrich, Steinheim, Germany) in dichloromethane (CH_2Cl_2 , analytical grade, Fisher Chemicals, Wholesaler in Schwerte, Germany) which was used freshly from the bottle. All DAT compounds were dissolved in dichloromethane (CH_2Cl_2) to a concentration of 0.3 mM.

Cyclic Voltammetry

The electrochemical experiments were carried out in a custom-made electrochemical cell that was air-sealed. Dichloromethane (CH₂Cl₂, Fisher Chemicals, analytical reagent grade) was used as solvent. All solutions were purged with argon 45 min before measurements. Cyclic voltammograms were recorded at 295 K using a potentiostat (Metrohm Autolab, Utrecht, Netherlands) with a three-electrode assembly comprising a glassy carbon (GC) disc as working electrode (WE, diameter $d=3$ mm), a Pt sheet as auxiliary electrode (Aux, $A=1$ cm²) and an Ag/Ag⁺ reference electrode filled with 0.01 M silver nitrate (Ref, AgNO₃, 99.9% p.a., Carl Roth, Karlsruhe, Germany) and 0.1 M Bu₄NClO₄ in acetonitrile (MeCN, Fisher Chemicals, HPLC grade). This electrode was calibrated with respect to the ferrocene/ferrocenium redox couple (Fc/Fc⁺) measured in solution with same concentration of supporting electrolyte and the same concentration of the Fc (0.3 mM) as the compound under investigation. All potentials are quoted with respect to the Fc/Fc⁺ couple.

UV/Vis and Fluorescence Spectroscopy

The absorption spectra were acquired using a Spekol 2000 (Analytik Jena, Jena, Germany) and fluorescence emission spectra were obtained using a FS5 spectrofluorometer (Edinburgh Instruments, Livingston, United Kingdom). All DAT compounds were dissolved in ethanol (analytical grade, Fisher Chemicals) to a concentration of 0.9 μM and measured against ethanol as reference. The same procedure was followed for the spectra in CH₂Cl₂.

Data Evaluation

The formal potentials E° were obtained as the arithmetic mean of the anodic (E_{pa}) and the cathodic (E_{pc}) peak potentials. The peak separation ΔE_p was determined as difference between E_{pa} and E_{pc} . For determining the ratio of anodic and cathodic peak currents I_{pa}/I_{pc} and I_{pc} value, Eq. (1) was used in which $I_{pc,0}$ is the uncorrected cathodic peak currents to the zero-current baseline and I_{λ} is the current at the vertex potential.

$$\frac{|I_{pc}|}{|I_{pa}|} = \frac{|I_{pc,0}|}{|I_{pa}|} + \frac{0.485 I_{\lambda}}{|I_{pa}|} + 0.086 \quad (1)$$

Theoretical Calculations

Density functional theory (DFT) calculations were performed on the B3LYP/6-31+G* level^[44-47] using Gaussian 16.^[48] The geometry of all structures was optimized for the ground and the excited states. Calculations for the excited states were carried out within time-dependent DFT. The ionization energies were obtained as energy differences between the neutral compound and the corresponding cations in their doublet states for which full geometry optimizations were made.

Acknowledgements

A.M. and L.B. gratefully acknowledge support by fellowships through the Graduate Programme "Nanoenergy" of the Ministry for Science and Culture of the State of Lower Saxony. Moreover, L.B. was member of the Graduiertenkolleg 1885 (DFG GRK1885) and A.M. is member of Graduiertenkolleg "Chemical Bond

Activation" (DFG GRK2226). The simulations were performed at the HPC Cluster CARL, located at the University of Oldenburg (Germany) and funded by the DFG through its Major Research Instrumentation Programme (INST 184/157-1 FUGG) and the Ministry of Science and Culture (MWK) of the State of Lower Saxony.

Conflict of Interest

The authors declare no conflict of interest.

Keywords: Diaminoterephthalates · fluorescence spectroscopy · UV/vis spectroscopy · fluorescence dyes · molecular electrochemistry

- [1] A. Baeyer, *Ber. Dtsch. Chem. Ges.* **1886**, *19*, 428.
- [2] L. I. Smith, R. L. Abler, *J. Org. Chem.* **1957**, *22*, 811.
- [3] H. Ulbricht, G. Löber, L. Kittler, *J. Prakt. Chem.* **1979**, *321*, 905.
- [4] H. Kauffmann, L. Weissel, *Justus Liebigs Ann. Chem.* **1912**, *393*.
- [5] J. Christoffers, *Eur. J. Org. Chem.* **2018**, 2366.
- [6] M. Xu, J.-M. Han, C. Wang, X. Yang, J. Pei, L. Zang, *ACS Appl. Mater. Interfaces* **2014**, *6*, 8708.
- [7] P. Y. Reddy, *Synthesis* **1998**, 999.
- [8] S. Girouard, M.-H. Houle, A. Grandbois, J. W. Keillor, S. W. Michnick, *J. Am. Chem. Soc.* **2005**, *127*, 559.
- [9] X.-D. Jiang, R. Gao, Y. Yue, G.-T. Sun, W. Zhao, *Org. Biomol. Chem.* **2012**, *10*, 6861.
- [10] I. Yapici, K. S. S. Lee, T. Berbasova, M. Nosrati, X. Jia, C. Vasileiou, W. Wang, E. M. Santos, J. H. Geiger, B. Borhan, *J. Am. Chem. Soc.* **2015**, *137*, 1073.
- [11] L. Yi, H. Li, L. Sun, L. Liu, C. Zhang, Z. Xi, *Angew. Chem. Int. Ed. Engl.* **2009**, *48*, 4034.
- [12] N. Wache, C. Schröder, K.-W. Koch, J. Christoffers, *ChemBioChem* **2012**, *13*, 993.
- [13] N. Wache, A. Scholten, T. Klüner, K.-W. Koch, J. Christoffers, *Eur. J. Org. Chem.* **2012**, 5712.
- [14] I. I. Senin, K.-W. Koch, M. Akhtar, P. P. Philippov, *Adv. Exp. Med. Biol.* **2003**, *514*, 69.
- [15] O. H. Weiergräber, I. I. Senin, E. Y. Zernii, V. A. Churumova, N. A. Kovaleva, A. A. Nazipova, S. E. Permyakov, E. A. Permyakov, P. P. Philippov, J. Granzin, K.-W. Koch, *J. Biol. Chem.* **2006**, *281*, 37594.
- [16] T. Gensch, K. E. Komolov, I. I. Senin, P. P. Philippov, K.-W. Koch, *Proteins* **2007**, *66*, 492.
- [17] S. Sulmann, M. Wallisch, A. Scholten, J. Christoffers, K.-W. Koch, *Biochemistry* **2016**, *55*, 2567.
- [18] J. C. Jewett, C. R. Bertozzi, *Chem. Soc. Rev.* **2010**, *39*, 1272.
- [19] M. Wallisch, S. Sulmann, K.-W. Koch, J. Christoffers, *Chem. Eur. J.* **2017**, *23*, 6535.
- [20] S. Leupold, T. Shokati, C. Eberle, T. Borrmann, F.-P. Montforts, *Eur. J. Org. Chem.* **2008**, *2008*, 2621.
- [21] H. Irngartinger, P. W. Fettel, T. Escher, P. Tinnefeld, S. Nord, M. Sauer, *Eur. J. Org. Chem.* **2000**, 455.
- [22] L. Freimuth, C. A. Rozzi, C. Lienau, J. Christoffers, *Synthesis* **2015**, *47*, 1325.
- [23] M. Prato, M. Maggini, *Acc. Chem. Res.* **1998**, *31*, 519.
- [24] S. Pittalis, A. Delgado, J. Robin, L. Freimuth, J. Christoffers, C. Lienau, C. A. Rozzi, *Adv. Funct. Mater.* **2015**, *25*, 2047.
- [25] D. Gust, T. A. Moore, A. L. Moore, *Acc. Chem. Res.* **2001**, *34*, 40.
- [26] G. D. Scholes, G. R. Fleming, A. Olaya-Castro, R. van Grondelle, *Nat. Chem.* **2011**, *3*, 763.
- [27] C. A. Rozzi, S. M. Falke, N. Spallanzani, A. Rubio, E. Molinari, D. Brida, M. Maiuri, G. Cerullo, H. Schramm, J. Christoffers, C. Lienau, *Nat. Commun.* **2013**, *4*, 1602.
- [28] L. Freimuth, J. Christoffers, *Chem. Eur. J.* **2015**, *21*, 8214.
- [29] M. H. Chisholm, N. J. Patmore, *Dalton Trans.* **2007**, 91.
- [30] J. Zhang, L. Huo, X. Wang, K. Fang, L. Fan, T. Hu, *Cryst. Growth Des.* **2017**, *17*, 5887.

- [31] I. Oyarzabal, B. Fernández, J. Cepeda, S. Gómez-Ruiz, A. J. Calahorra, J. M. Seco, A. Rodríguez-Diéguez, *CrystEngComm* **2016**, *18*, 3055.
- [32] G. Wittstock, S. Rastgar, S. Scarabino, *Curr. Opin. Electrochem.* **2019**, *13*, 25.
- [33] G. Dryhurst, K. M. Kadish, F. Scheller, R. Renneberg, *Biological Electrochemistry*, Academic Press, London, **1982**.
- [34] P. S. Guin, S. Das, P. C. Mandal, *Int. J. Electrochem.* **2011**, *1*.
- [35] C. Rüssel, W. Jaenicke, *J. Electroanal. Chem.* **1986**, *200*, 249.
- [36] M. Shamsipur, A. Siroueinejad, B. Hemmateenejad, A. Abbaspour, H. Sharghi, K. Alizadeh, S. Arshadi, *J. Electroanal. Chem.* **2007**, *600*, 345.
- [37] Z.-Q. Wu, X.-K. Jiang, S.-Z. Zhu, Z.-T. Li, *Org. Lett.* **2004**, *6*, 229.
- [38] M. Penning, J. Christoffers, *Eur. J. Org. Chem.* **2012**, 1809.
- [39] L. Buschbeck, J. Christoffers, *J. Org. Chem.* **2018**, *83*, 4002.
- [40] R. Jimmidi, G. K. Shroff, M. Satyanarayana, B. R. Reddy, J. Kapireddy, M. A. Sawant, S. L. Sitaswad, P. Arya, P. Mitra, *Eur. J. Org. Chem.* **2014**, 1151.
- [41] K. Pachamuthu, X. Zhu, R. R. Schmidt, *J. Org. Chem.* **2005**, *70*, 3720.
- [42] L. Buschbeck, *PhD Thesis*, Carl von Ossietzky Universität Oldenburg, Oldenburg, **2018**.
- [43] L. Freimuth, *PhD Thesis*, Carl von Ossietzky Universität of Oldenburg, Oldenburg, **2016**.
- [44] A. D. Becke, *J. Chem. Phys.* **1993**, *98*, 5648.
- [45] C. Lee, W. Yang, R. G. Parr, *Phys. Rev. B* **1988**, *37*, 785.
- [46] S. H. Vosko, L. Wilk, M. Nusair, *Can. J. Phys.* **1980**, *58*, 1200.
- [47] P. J. Stephens, F. J. Devlin, C. F. Chabalowski, M. J. Frisch, *J. Phys. Chem.* **1994**, *98*, 11623.
- [48] M. J. Frisch, G. W. Trucks, H. B. Schlegel, G. E. Scuseria, M. A. Robb, J. R. Cheeseman, G. Scalmani, V. Barone, G. A. Petersson, H. Nakatsuji, X. Li, M. Caricato, A. V. Marenich, J. Bloino, B. G. Janesko, R. Gomperts, B. Mennucci, H. P. Hratchian, J. V. Ortiz, A. F. Izmaylov, J. L. Sonnenberg, D. Williams-Young, F. Ding, F. Lipparini, F. Egidi, J. Goings, B. Peng, A. Petrone, T. Henderson, D. Ranasinghe, V. G. Zakrzewski, J. Gao, N. Rega, G. Zheng, W. Liang, M. Hada, M. Ehara, K. Toyota, R. Fukuda, J. Hasegawa, M. Ishida, T. Nakajima, Y. Honda, O. Kitao, H. Nakai, T. Vreven, K. Throssell, J. A. Montgomery, J. E. Peralta, F. Ogliaro, M. J. Bearpark, J. J. Heyd, E. N. Brothers, K. N. Kudin, V. N. Staroverov, T. A. Keith, R. Kobayashi, J. Normand, K. Raghavachari, A. P. Rendell, J. C. Burant, S. S. Iyengar, J. Tomasi, M. Cossi, J. M. Millam, M. Klene, C. Adamo, R. Cammi, J. W. Ochterski, R. L. Martin, K. Morokuma, O. Farkas, J. B. Foresman, D. J. Fox, *Gaussian, Inc.*, Wallingford CT, **2016**.

Manuscript received: April 17, 2019
